DOI: https://doi.org/10.15407/techned2023.04.062

MODELING OF A CONTROLLED ELECTROMAGNETIC VIBRATION DRIVE WITH A VARIABLE RESONANT FREQUENCY

O.O. Cherno*, A.Yu. Kozlov
Admiral Makarov National University of Shipbuilding,
Heroiv Ukrainy Ave, 9, Mykolaiv, 54007, Ukraine.
E-mail: alextcherno@gmail.com.

The technology for the production of high-quality concrete products includes the vibration of the concrete mixture at various frequencies. For this, an electromagnetic vibration drive can be used, which has high reliability, durability and controllability. For its effective application, it is necessary to adjust the resonance frequency of the oscillating system in order to ensure the near-resonance mode of operation at different frequencies. This is possible by using devices with adjustable stiffness, in particular, controlled dynamic vibration absorbers with nonlinear elastic elements. In the article the electromagnetic, electromechanical, mechanical, and energy processes in a controlled vibration system, which includes an electromagnetic vibrator and a vibration absorber with conical springs, the stiffness of which is regulated by compression using a press, have been investigated. Using the circle-field method, a mathematical and simulation model of electromagnetic and electromechanical processes in the vibrator has been developed. For this purpose, numerical calculations of the magnetic field in the vibrator have been performed and, based on the obtained results, the functional dependences between the electromagnetic force, magnetic flux, magnetomotive force and the size of the air gap have been determined. A model of the mechanics of the oscillating system, processes in the vibration absorber press drive and processes in the control system has been also developed. The built simulation models were combined into a general model in the Simulink environment, by means of which the time diagrams of the processes have been obtained. The modeling results show that the system provides a smooth transition from one vibration frequency to another while maintaining the specified amplitude of the working body oscillations and near-resonance mode with high energy efficiency. References 12, figures 10, tables 3.
Keywords: electromagnetic drive; vibrating device; controlled vibration absorber; automatic control.

Introduction. Vibrating equipment is used for many technological processes, in particular, for compaction of concrete mixtures. One of the ways to improve the quality of concrete products is to apply sequential vibrations at different frequencies. This makes it possible to improve the compaction of stones of different sizes in the concrete mix: large crushed stone fractions are better compacted at low frequencies and the small ones − at high frequencies [1]. Today, regulation of the vibration frequency is implemented mainly with the help of a frequency-controlled unbalanced vibration drive [2, 3]. But when working at high frequencies, it has rapid wear of mechanical components, particularly of bearings [4]. The electromagnetic drive, which is able to work in a wide range of frequencies and has high reliability and durability [4, 5], is devoid of this drawback. But, for its effective use, it is necessary that it works in a mode close to resonance [6]. To ensure such a mode at different frequencies, it is necessary to use elements with adjustable stiffness, by means of which the resonant frequency of the system can be changed according to the vibration frequency. This can be done by the controlled dynamic vibration absorbers installed on the intermediate mass of the vibration devices [6], in particular, it can be vibration absorber with conical springs [7]. To provide the operation of such a system, it is necessary to ensure compatible control of the frequency and amplitude of the electromagnetic drive and the stiffness of the vibration absorber springs, which requires taking into account the peculiarities of electromagnetic and mechanical processes during their interaction. Therefore, the study of these processes in order to control them is an actual problem.

Analysis of previous studies. In different works the processes in vibration devices were investigated when applying various algorithms for the simultaneous control of an electromagnetic drive and an electromagnetic dynamic vibration absorber. In [6] a control algorithm that can be used to implement sequential vibration at different frequencies is considered. That is, when the vibration frequency is not adjusted to the resonant frequency of the device, but is set by an external signal, and the task of controlling the vibration absorber is not to achieve anti-resonance of the intermediate mass, but to ensure resonance mode of the drive operation. When modeling electromagnetic and electromechanical processes in the

* ORCID ID: https://orcid.org/0000-0003-1670-8276

vibrator, the circle-field method was used in [6], and the method of conformal transformations was used for the vibration absorber modelling.

The use of non-linear elastic elements to change mechanical stiffness makes it possible to use larger values of the reactive mass than with electromagnetic control [7], which expands the scope of application of such systems to larger vibrating devices. However, vibration absorbers with nonlinear elastic elements, in particular, with conical springs, unlike electromagnetic ones, have a significant adjustment time. This is due to the necessity of the elastic elements compression to achieve the necessary value of their stiffness [7]. Therefore, the processes for the simultaneous control of vibration absorbers of this type and the vibration drive can fundamentally differ from those described in [6], where only electromagnetic devices are considered.

The goal of the work. The purpose of this work is the research of electromagnetic, electro-mechanical, mechanical and energy processes in a resonant vibration system, which contains a frequency and amplitude controlled electromagnetic drive and a controlled dynamic vibration absorber with conical springs, which operates in the mode of sequential vibration at different frequencies.

The general structure of the vibrating device. Let's take as a basis a vibrating device for compacting concrete mixtures, which is used as an experimental stand in the laboratory of the Admiral Makarov National University of Shipbuilding. Its functional scheme is shown in Fig. 1. Notations defined in this scheme: *1* is the working body of the vibration device; *2* is the electromagnetic vibrator; *3* is the intermediate mass; *4* is the controlled dynamic vibration absorber with conical springs; *5* is the relay device for commutation of the motor coils of the vibration absorber press electric drive; *6* is the a transistor converter with PWM powering the coils of the electromagnetic vibrator; *7* is the control system; *8* is the vibrator coil current sensor; *9* is the accelerometer installed on the working body.

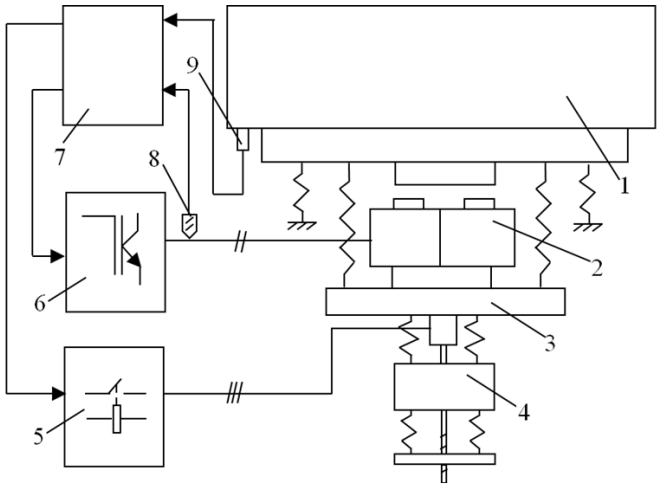

Fig. 1

The device works as follows. As a result of processing the signals of the accelerometer and the current sensor in the control system, the amplitude of the working body oscillations and their phase relative to the electromagnetic force are determined. This information is used to control the amplitude and frequency of the current in the vibrator coils, providing oscillation with given amplitude at the resonant frequency. If it is necessary to change the vibration frequency, the vibration absorber press is set in motion. It changes the value of initial compression of the conical springs, changing their stiffness and, accordingly, the resonant frequency of the system. In response to this, the frequency control system changes the frequency of the forced oscillations, adjusting to the new resonance. Thus, the vibration amplitude and frequency are controlled while maintaining the energy-efficient resonant mode of operation.

Model of electromagnetic and electromechanical processes. The parameters of the electromagnetic vibrator are listed in Table 1.

Table 1

Number of the electromagnets n_{elmagn}		2	Electrical steel	3413
Number of the electromagnet coil turns W		612	The shape of the core and of the armature	U
Connection of the coils		parallel	Length of the core and of the armature, mm	45
The initial value of the air gap size δ, mm		1.9	Core height, mm	76
Active resistance of the electromagnet coil R, Ohm		2	Armature height, mm	75
Parameters of the electromagnet equivalent circuit [6], characterizing losses in steel, kOhm	$R^*_{e.c}$	14.7	Pole width, mm	25
	$R^*_{h.st}$	34	Distance between poles, mm	39

Let's use the circle-field method to simulate processes in the electromagnet. It is based on the approximation of the dependences of the flux coupling and the electromagnetic force on the magnetomotive force and the size of the air gap, obtained by numerical calculations of the magnetic field [8, 9]. To do this, we build a model of an electromagnet in the specialized Ansoft Maxwell program, in which for a number of combinations of magnetomotive force values and the size of the air gap, we calculate the flux coupling and the electromagnetic force using the formulas:

$$\psi = \sum_{j=1}^{W} \int_{S_{wj}} \mathbf{B}\mathbf{n}_{wj} dS_{wj} \; ; \; F_e = \frac{1}{\mu_0} \oint_S \left((\mathbf{Bn})\mathbf{B} - \frac{1}{2} B^2 \mathbf{n} \right) dS \, ,$$

where S_{wj} is the area of the j-th turn of the coil; **B** is the magnetic induction vector; $\mathbf{n}_{wj}$ is the normal to the plane of the j-th coil turn; S is the armature surface; **n** is a the normal vector to the surface of the armature**.** The resulting dependencies are presented in Fig. 2.

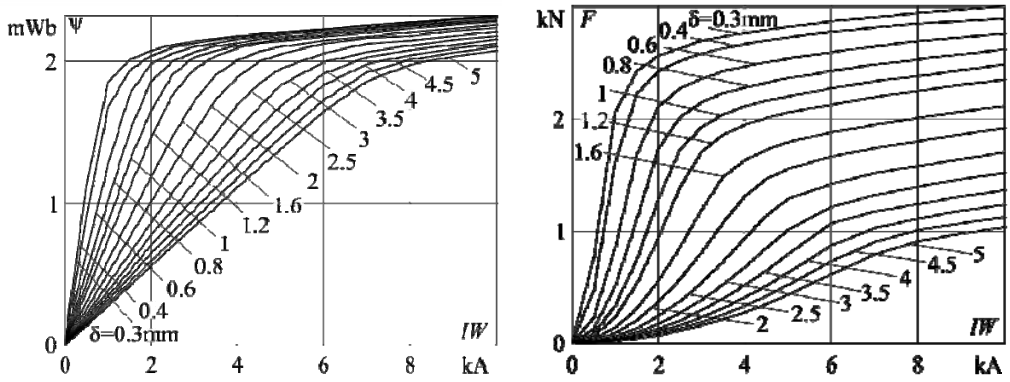

Fig. 2

In order for the dependences between magnetomotive force IW and flux coupling ψ to be used for modeling dynamics, they must be reduced to $IW(\psi)$ functions [6]. For this purpose, let's use the method used in [10]. We approximate the obtained dependences $\psi_j(IW)$ by hyperbolic functions:

$$y_j(x) = \left(y_{c_j} - k_{r_j} x_{c_j} \right) \left(1 - \sqrt{\frac{\left(x - x_{c_j} \right)^2 + b_j^{\,2}}{x_{c_j}^2 + b_j^2}} \right) + k_{r_j} x \, ,$$

where j is the dependency number corresponding to a certain value of the air gap size; (x_c, y_c) are the coordinates of the hyperbola center; b is the value specifying the focal length; k_r is the rotation ratio.

For the dependence $\psi_7(IW)$ which corresponds to the size of the air gap δ = 1.6 mm, we determine the coefficients of the approximating function by the method of least squares by sorting through four nested loops and find the slope coefficient of the upper asymptote:

$$k_a = \frac{k_{r_7} x_{c_7} - y_{c_7}}{\sqrt{x_{c_7}^2 + b_7^2}} + k_{r_7} = 2.465 \cdot 10^{-8} \text{ Wb/A}.$$

This coefficient will be the same for all hyperbolas $y_j(x)$. Therefore, for other values of j, we perform an enumeration of only the values of x_c, y_c and b, and the coefficient k_r is determined by the formula:

$$k_r = \left(y_c (x_c^2 + b^2)^{-1/2} + k_a \right) \left(x_c (x_c^2 + b^2)^{-1/2} + 1 \right)^{-1} .$$

As a result, we get the coefficients of the approximating functions listed in Table 2.

Table 2

j	1	2	3	4	5	6	7	8	9	10	11	12	13	14
δ, mm	0.3	0.4	0.6	0.8	1	1.2	1.6	2	2.5	3	3.5	4	4.5	5
x_c, kA	0.829	1.037	1.53	1.95	2.34	2.75	3.44	4.07	4.74	5.3	5.86	6.34	6.8	7.18
y_c, mWb	2.113	2.116	2.118	2.116	2.116	2.116	2.11	2.105	2.093	2.077	2.071	2.052	2.043	2.027
b, kA	0.355	0.440	0.506	0.567	0.63	0.67	0.764	0.790	0.919	1.01	1.105	1.065	1.115	1.084
k_r,mWB/kA	1.234	0.991	0.687	0.544	0.457	0.392	0.316	0.269	0.231	0.207	0.188	0.173	0.162	0.153

For a range of fixed flux linkage values Ψ = 0, 0.1 ... 2.5 (mWb) we create the equation:

$$\psi_j(IW) = \Psi_k,$$

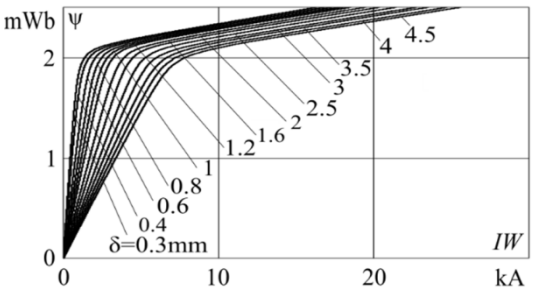

Fig. 3

where k = 1..26. Using the bisection method, we obtain a number of magnetomotive force values $IW_{j,k}$, which correspond to the set values of flux coupling Ψ_k at the values of the air gap δ_j. By interpolation we get a family of functions $IW_j(\psi)$, the graphs of which are shown in Fig. 3.

Derived dependencies $IW(\psi,\delta)$ and $F_e(IW,\delta)$ enter in the appropriate blocks "IW" and "Magnetic force" of the simulation model of the electromagnet in the Simulink environment (Fig. 4).

Using the electromagnet equivalent circuit [6], which takes into account the influence of eddy currents and hysteresis, we create the equations of electromagnetic processes:

$$i(t) = \frac{1}{W} IW\left(\psi(t), \delta(t)\right) + i_h^*(t) + i_{e.c}^*(t); \quad \frac{d\psi}{dt} = u(t) - Ri(t), \qquad (1), (2)$$

$$i_{e.c}^*(t) = \frac{1}{R_{e.c}^*}\left(u(t) - Ri(t)\right); \quad i_h^*(t) = \frac{f_{I.st}}{R_{h.st}^* f_I(t)}\left(u(t) - Ri(t)\right), \qquad (3), (4)$$

where $i_{e.c}^* = i_{e.c}/W$; $i_h^* = i_h/W$; $R_{e.c}^* = R_{e.c}W^2$; $R_{h.st}^* = R_{h.st}W^2$; i is a coil current; f_I is a current frequency; $i_{e.c}$ is a magnetomotive force, which is created by eddy currents; i_h is a magnetomotive force, which determines the reactive component of magnetization; $R_{e.c}$ is a equivalent resistance of eddy current circuit; $R_{h.st}$ is a fictitious resistance characterizing hysteresis losses at standard current frequency $f_{I.st}$, for which loss reference data is provided. Based on these equations we create a simulation model of electromagnetic and electromechanical processes, shown in Fig. 4.

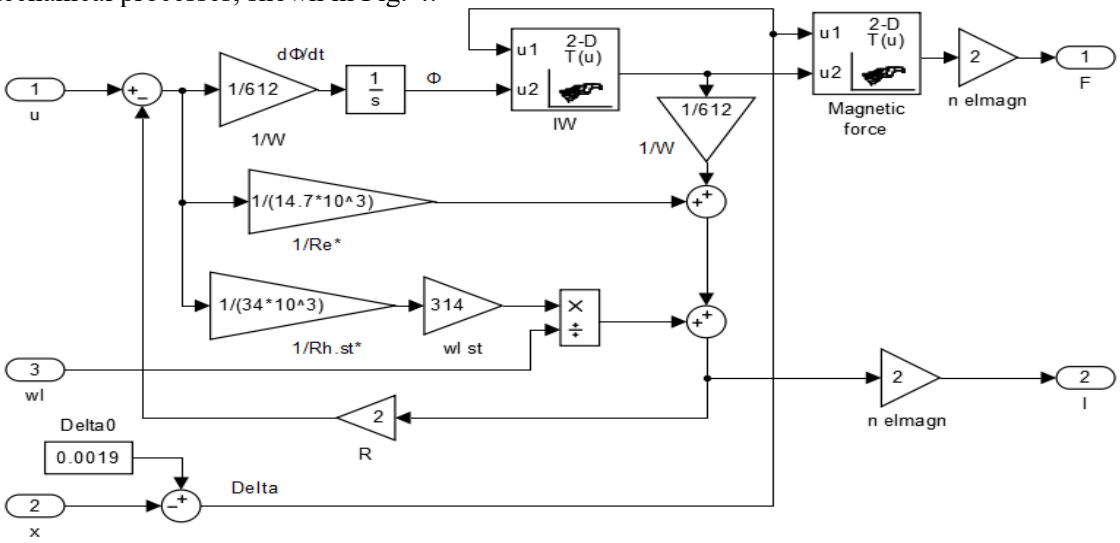

Fig. 4

The model works as follows. The instantaneous value of the coil voltage is applied to the "u" input, the voltage drop across the active resistance is subtracted from it and determined electromotive force, which is divided by the number of coil turns to obtain the time derivative of the magnetic flux. Then it is integrated to determine the magnetic flux, which enters the input of the "IW" block, where the interpolation of the dependence $IW(\Phi, \delta)$ is performed. The second input of the "IW" block receives the value of the air gap, and at its output we get the magnetomotive force, which enters the input of the "Magnetic force" block, which calculates the electromagnetic force. According to the equation (1), the current in the electromagnet coil is determined. Then it is multiplied by the active resistance and the voltage drop across it is determined. The value of the armature movement relative to the core enters the input "*x*". It is subtracted from the initial value of the air gap and the current value of δ is determined. It enters the second inputs of the "IW" and "Magnetic force" blocks.

The model of the oscillating system mechanics and processes in the drive of the vibration absorber press. Figure 5 shows the mechanics diagram of the oscillating system, the diagram of the vibration absorber with conical springs, and the stiffness characteristic of the spring. Notations defined in the figure: $m_0...m_2$ are the mass of the working body, the intermediate platform and the moving part of the vibration absorber; $c_0...c_2$ are the stiffness of shock absorbers, springs in the suspension of the intermediate platform and springs of the vibration absorber; $b_0...b_2$ are loss coefficients in the corresponding springs; m_3, c_3 and b_3 are the parameters reflecting the inertial, elastic and dissipative properties of the concrete mixture [11]; *1* is the DC motor; *2* is the reducer; *3* is the moving part of the vibration absorber; *4* is the conical springs; *5* is the press; *6* is the helical gear; x_1, x_2, x_{pr} are the moving the intermediate platform, vibration damping mass and the press; $F_{spr}(\Delta x)$ is a reaction force of a conical spring depending on its deformation.

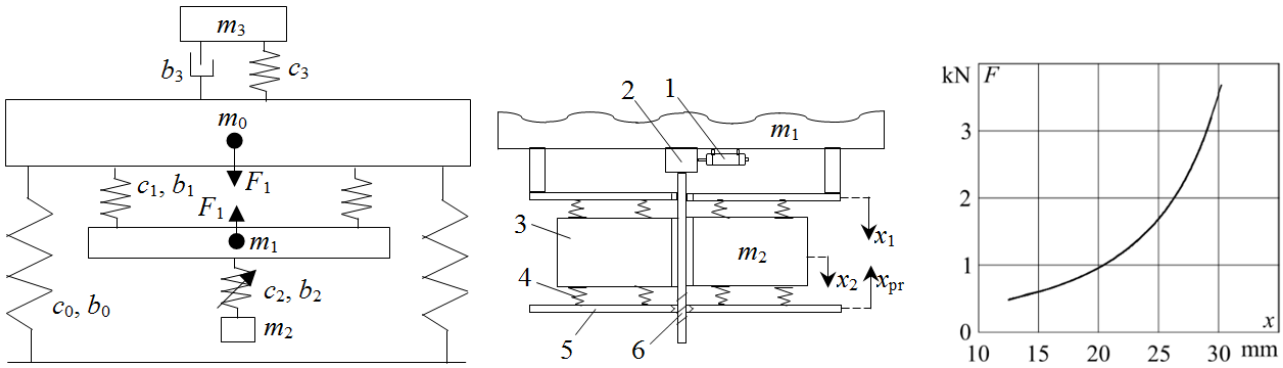

Fig. 5

The values of the mechanics diagram parameters and the characteristics of the vibration absorber press drive are given in Table 3.

Table 3

Parameters of the mechanics diagram											
m_0	m_1	m_2	m_3	c_0	c_1	c_2	c_3	b_0	b_1	b_2	b_3
kg				MN/m				N·s/m			
149	41	10	10	1.45	8.96	0.5..1.5	1	43.5	610	48	1700

Characteristics of the vibration absorber press drive						
Type of drive motor	Electrical time constant T_e, s	Mechanical time constant T_m, s	Motor voltage constant K_m, $(\text{V·s})^{-1}$	Motor torque constant K_t, $(\text{N·m·s})^{-1}$	Gear ratio of the reducer i_r	Screw pitch h, m
УЛ-042-18	0.01	0.09	9.615	1202	741	0.005

For the convenience of modeling, the characteristic of the conical spring can be approximated in the working area Δx = 0.013..0.03 m by a polynomial [7]:

$$F_{spr}(\Delta x) = \sum_{i=0}^{5} a_i \cdot (\Delta x \cdot 10^3)^i , \tag{5}$$

where $a_0 = -1.02 \cdot 10^4$ N; $a_1 = 2.842 \cdot 10^3$ N/m; $a_2 = -302.762$ N/m^2; $a_3 = 16.086$ N/m^3; $a_4 = -0.422$ N/m^4; $a_5 = 4.479 \cdot 10^{-3}$ N/m^5.

Based on the diagrams in Fig. 5 we create the equations of the oscillating system mechanics:

$$\frac{dv_0}{dt} = \frac{1}{m_0}\Big(F_1(t) - b_0 v_0(t) - b_1 \cdot (v_0(t) - v_1(t)) - b_3 \cdot (v_0(t) - v_3(t)) - c_0 x_0(t) - c_1 \cdot (x_0(t) - x_1(t)) - c_3 \cdot (x_0(t) - x_3(t))\Big); \tag{6}$$

$$\frac{dv_1}{dt} = \frac{1}{m_1}\Big(-F_1(t) + b_1 \cdot (v_0(t) - v_1(t)) - b_2 \cdot (v_1(t) - v_2(t)) + c_1 \cdot (x_0(t) - x_1(t)) - F_2(t)\Big); \tag{7}$$

$$\frac{dv_2}{dt} = \frac{1}{m_2}\Big(F_2(t) - b_2 \cdot (v_2(t) - v_1(t))\Big); \quad \frac{dv_3}{dt} = \frac{1}{m_3}\Big(b_3 \cdot (v_0(t) - v_3(t)) + c_3 \cdot (x_0(t) - x_3(t))\Big); \tag{8), (9}$$

$$\frac{dx_i}{dt} = v_i(t), i = 0..3; \tag{10}$$

$$F_2(t) = 4F_{spr}\left(x_1(t) - x_2(t) + \frac{1}{2}x_{pr}(t)\right) - 4F_{spr}\left(x_2(t) - x_1(t) + \frac{1}{2}x_{pr}(t)\right). \tag{11}$$

Based on these equations, we build a simulation model of mechanical processes in the oscillating system in the Simulink environment (Fig. 6).

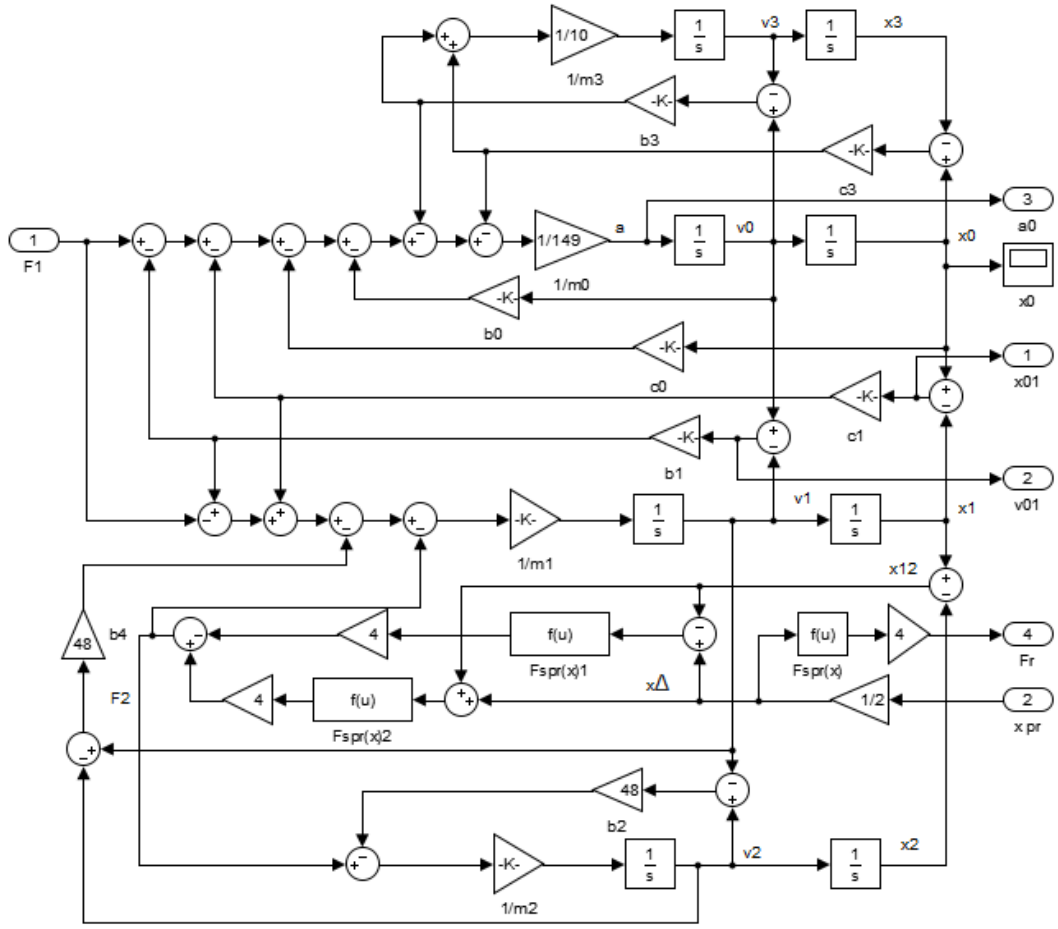

Fig. 6

The press drive of the vibration absorber with conical springs, which is used in the considered system, contains a direct current motor УЛ-042-18, reducer and helical gear (Table 3).

The motor speed without load $\omega_{m.idl}$ is determined by the differential equation:

$$T_e T_m \frac{d^2\omega_{m.idl}}{dt^2} + T_m \frac{d\omega_{m.idl}}{dt} + \omega_{m.idl}(t) = k_m u_m(t), \tag{12}$$

where u_m is the input voltage.

The reaction force of conical springs when they are compressed by a press:

$$F_r(t) = 4F_{spr}\left(\frac{1}{2}x_{pr}(t)\right). \tag{13}$$

This force creates a resistance torque acting on the motor rotor:

$$M_r(t) = \frac{h}{i_r \eta_{gear}} F_r(t), \tag{14}$$

where η_{gear} is the efficiency of the mechanism, which takes into account losses in the reducer and helical gear.

When the press moves, the resistance torque causes a decrease in the rotation frequency by the value of $\Delta\omega_m$, which is determined by the differential equation:

$$T_e T_m \frac{d^2 \Delta\omega_m}{dt^2} + T_m \frac{d\Delta\omega_m}{dt} + \Delta\omega_m(t) = k_t \cdot \left(T_m \frac{dM_r}{dt} + M_r(t) \right). \quad (15)$$

A peculiarity of helical transmission is a sliding friction, which at low speeds has a significantly nonlinear characteristic [12]. But in this model this nonlinearity can be neglected. It is enough to take into account only the fact that the reaction force of the springs cannot cause the screw to rotate in the direction opposite to the torque created by the motor. That is, the movement of the motor, screw and press occurs when the frequency $\omega_{m.idl}$ exceeds the value $\Delta\omega_m$, or when they are directed in the same direction (during the reverse movement of the press). Thus, the motor shaft rotation frequency will be determined by the following equation:

$$\omega_m(t) = \begin{cases} \omega_{m.idl}(t) - \Delta\omega_m(t) \text{ if } (\omega_{m.idl}(t) > \Delta\omega_m(t)) \vee (\omega_{m.idl}(t) < -\omega_{\min}); \\ 0 \text{ otherwise,} \end{cases} \quad (16)$$

where $\omega_{\min}$ is the minimum angular velocity sufficient to overcome the force of viscous friction.

On the basis of equations (12) − (16), we build a simulation model of the vibration absorber press drive in the Simulink environment in the form of the "Vibroabsorber drive system" subsystem (Fig. 7).

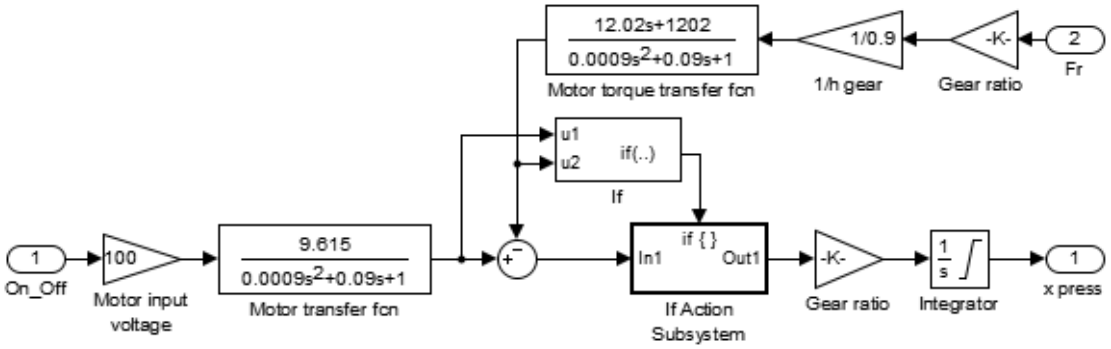

Fig. 7

A control signal is sent to the "On_Off" input, which can take the value −1, 0 or 1. The output of the subsystem is the calculated value of the movement of the press x_{pr}, taking into account the resistance force and the characteristics of the drive.

Model of processes in the control system. The simulation model of the electromagnetic vibration drive control system was developed in [6]. In [11] it is represented by a separate Control system subsystem. We add to this subsystem the control circuit of the vibration absorber press (Fig. 8).

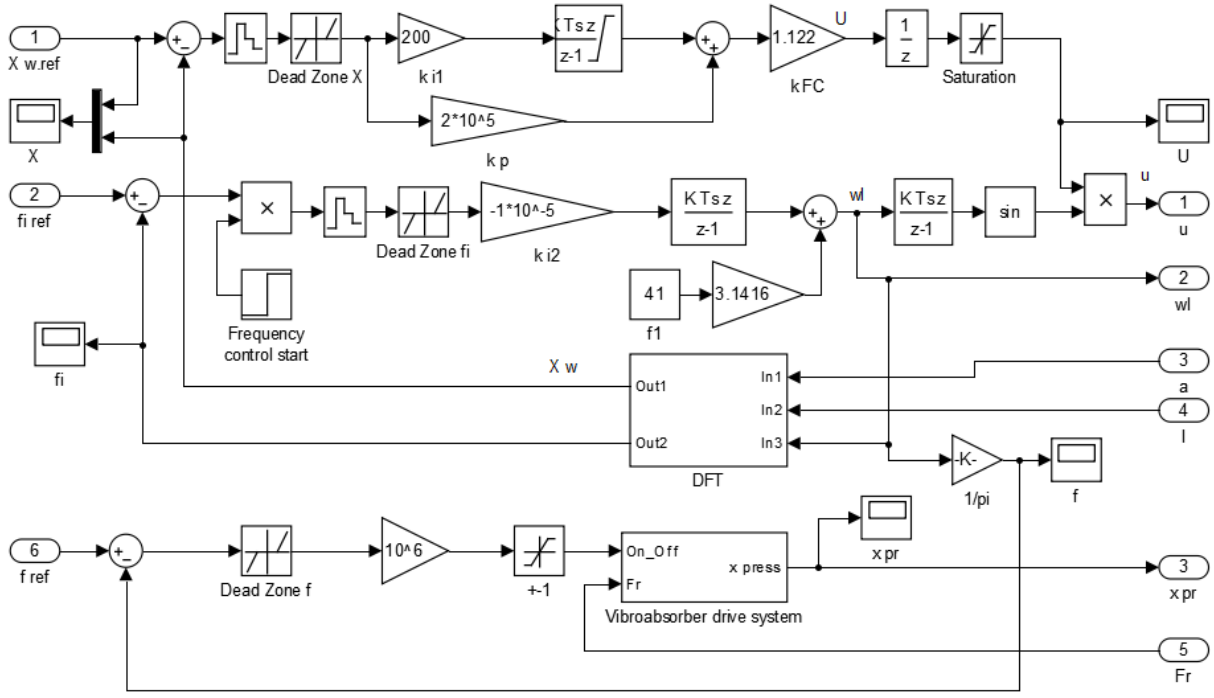

Fig. 8

The input signal of the press control circuit is the assigned value of the vibration frequency f_{ref}, which is compared with its real value f. If the difference between them (error) exceeds the value of the insensitivity zone specified by the "Dead zone f" block, 1 or −1 is applied to the "On_Off" input, depending on the sign of the error.

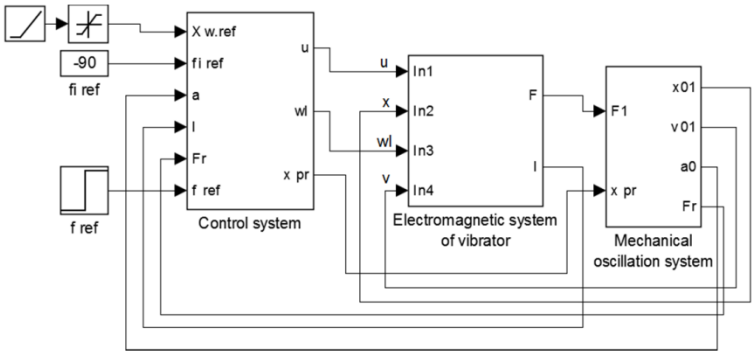

Fig. 9

Simulation results. The complete simulation model of the controlled vibration system is shown in Fig. 9. It consists of three subsystems: "Control system", "Electromagnetic system of vibrator" and "Mechanical oscillation system". The structure of the first one is shown in Fig. 8, the second one − in Fig. 4, the third one − in Fig. 6.

The input signals are the reference values of the working body oscillation amplitude $X_{w.ref}$, the vibration frequency f_{ref} and the phase shift between the electromagnetic force and the movement of the working body φ_{ref}. To maintain the resonant mode, the value $\varphi_{ref} = -90°$ is set.

The Figure 10 shows the result of the simulation: the time diagrams of the working body vibration amplitude X_w (the reference value and the real one), the frequency of vibration f, the phase shift between the electromagnetic force and the movement of the working body φ, the movement of the press x_{pr}, the output (mechanical) power of the vibrator P_{out}, the efficiency of the vibrator η.

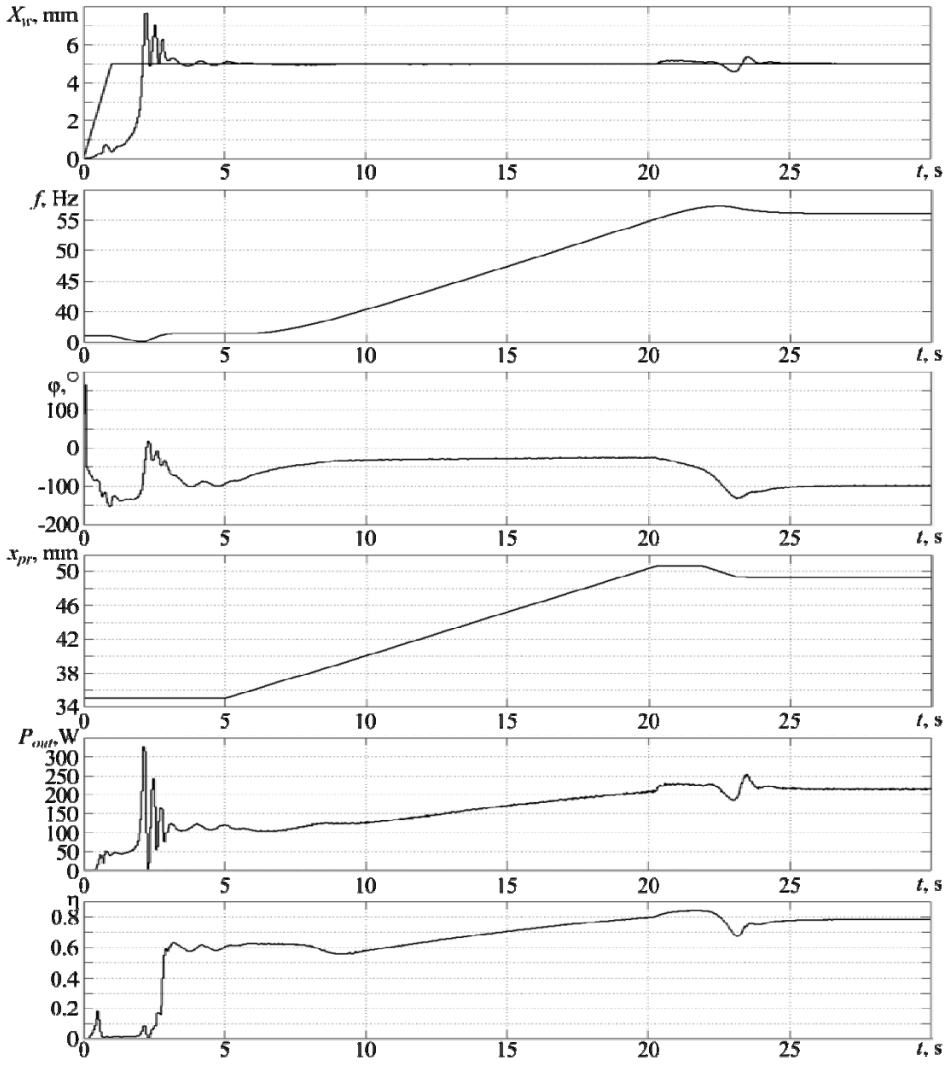

Fig. 10

The graphs show the following processes. The drive starts with a frequency of 41 Hz. The reference amplitude value $X_{w.ref}$ increases linearly to 0.5 mm within 1 s and then remains at this level. At a time of 1 s, the automatic frequency adjustment system is turned on, at a time of 3.2 s it sets a frequency of 41.4 Hz, which corresponds to resonance ($\varphi \approx -90°$). At the moment of 3.3 s, the oscillatory transient process of adjusting the vibration amplitude is finished, the amplitude value reaches the reference one and does not deviate from it by more than 5%. At a time of 5 s, a new reference value of frequency $f_{ref} = 61$ Hz is set. The difference in frequencies f_{ref} and f goes beyond of the dead zone ±1 Hz, and the press movement drive is turned on. The movement of the press is accompanied by compression of the conical springs, an increase in their stiffness and the resonant frequency of the oscillating system. In response to this, the automatic frequency adjustment system increases the frequency of forced oscillations f. As a result, the frequency increases smoothly and after a small overshoot is set at the level of 61.05 Hz. The press drive corrects the frequency error, after which it stops. This is also accompanied by a single fluctuation of the vibration amplitude within ±0.4 mm for 2 seconds. After that stationary vibrations are established at a new frequency with given amplitude.

The output power and efficiency of the vibrator have been calculated according to the method described in [6]. The simulation results show that the drive maintains high energy efficiency when switching between frequencies. An increase in the frequency at an unchanged vibration amplitude leads to an increase in the output power and, as a result, to an increase in the efficiency of the vibrator from 0.62 to 0.78.

Conclusions. The processes in the controlled electromagnetic drive of the vibration device, which contains an autoparametric vibration absorber with nonlinear elastic elements, have been investigated by means of simulation modeling. It was established that the simultaneous control of the electromagnetic vibrator and the dynamic vibration absorber ensures the consistent operation of the vibration device at different frequencies while maintaining the energy-efficient near-resonance mode. The transition from one frequency to another occurs smoothly, the transition time is determined by the dynamic properties of the absorber press drive. For the considered drive the transition speed is about 1.5 Hz per second.

1. Ratushnyak H.S., Slobodian N.M. Vibro-force technology of forming decorative concrete products. Vinnytsia: Universum-Vinnytsia, 2007. 161 p. (Ukr).

2. Chubik R.V., Yaroshenko L.V. Controlled vibration technological machines. Vinnytsia: VNAU, 2011. 355 p. (Ukr).

3. Nozhenko V., Rodkin D., Tytiuk V., Bohatyrov K., Burdilna E., Ilchenko O. Features of the Control Actions Formation During the Start-up of Vibration Machines at Passing of the Resonance Zone. Proceedings of the 25th IEEE International conference on *Problems of automated electric drive. Theory and practice (PAEP)*. Kremenchuk, Ukraine, 21-25 September 2020. Pp. 18–21. DOI: https://doi.org/10.1109/PAEP49887.2020.9240835.

4. Lanets O.S. High efficiency interresonance vibrating machines with electromagnetic drive (Theoretical foundations and building practice). Lviv: NULP, 2008. 324 p. (Ukr).

5. Despotovic Z., Stojilkovic Z. Power converter control circuits for two-mass vibratory conveying system with electromagnetic drive: simulations and experimental results. *IEEE Transactions on Industrial Electronics*. 2007. Vol. 54. No 1. Pp. 453–466. DOI: https://doi.org/10.1109/tie.2006.888798.

6. Cherno O.O. Energy efficient controlled electromagnetic drive systems of vibration equipment. Theory and practice: author's abstract of Dr. tech. sci. diss.: 05.09.03. Kremenchuk Mykhailo Ostrogradskiy National University Ministry of Education and Science of Ukraine. Kremenchuk. 2020. 36 p. (Ukr)

7. Cherno O.O., Krutyakova O.O. Synthesis of a digital regulator of the automatic control system of a dynamic vibration absorber with nonlinear elastic elements. *Zbirnyk naukovykh prats NUK*. 2010. No 2. Pp. 104–111. (Ukr).

8. Vaskovskii Yu.N. Prospects for modeling dynamic modes of electromechanical converters based on chain-field methods. *Elektrotekhnika i Elektromekhanika*. 2003. No 1. Pp. 23–25. (Rus).

9. Neyman L., Neyman V., Shabanov A. Vibration dynamics of an electromagnetic drive with a half-period rectifier. Proc. of 18-th International Conference *Micro/nanotechnologies and Electron Devices EDM*. Erlagol, Russia, 29 June – 03 July 2017. Pp. 503−506. DOI: https://doi.org/10.1109/edm.2017.7981805.

10. Cherno O.O., Gerasin O.S., Topalov A.M., Stakanov D.K., Hurov A.P., Vyzhol Yu.O. Simulation of mobile robot clamping magnets by circle-field method. *Tekhnichna elektrodynamika*. 2021. No 3. Pp. 58–64. DOI: https://doi.org/10.15407/techned2021.03.058.

11. Cherno O.O., Hurov A.P., Novogretskyi S.M. Peculiarities of the dynamics of the controlled electromagnetic drive of the vibration unit for compaction of concrete mixtures. *Avtomatyzatsiia vyrobnychykh protsesiv u mashinobuduvanni ta pryladobuduvanni*. 2014. Issue 48. Pp. 87−96. (Ukr).

12. Buryakovskyi S.G., Maslii A.S., Asmolova L.V., Honcharuk N.T. Mathematical modelling of transients in the electric drive of the turnout of the mono-sleeper type with switched-inductor motor. *Elektrotekhnika i Elektromekhanika*. 2021. No 2. Pp. 16−22. (Ukr). DOI: https://doi.org/10.20998/2074-272X.2021.2.03.

УДК 621.3:681.5

МОДЕЛЮВАННЯ КЕРОВАНОГО ЕЛЕКТРОМАГНІТНОГО ВІБРАЦІЙНОГО ПРИВОДА ЗІ ЗМІННОЮ РЕЗОНАНСНОЮ ЧАСТОТОЮ

О.О. Черно, докт. техн. наук, **А.Ю. Козлов**
Національний університет кораблебудування ім. адмірала Макарова,
просп. Героїв України, 9, Миколаїв, 54007, Україна.
E-mail: alextcherno@gmail.com.

Технологія виробництва високоякісних бетонних виробів включає в себе вібрування бетонної суміші на різних частотах. Для цього може бути використаний електромагнітний вібраційний привод, який має високу надійність, довговічність та керованість. Для його ефективного застосування необхідно здійснювати регулювання резонансної частоти коливальної системи з метою забезпечення білярезонансного режиму роботи на різних частотах. Це можливо шляхом використання пристроїв з регульованою жорсткістю, зокрема, керованих динамічних віброгасників з нелінійними пружними елементами. У роботі досліджено електромагнітні, електромеханічні, механічні та енергетичні процеси у керованій вібраційній системі, що містить електромагнітний вібратор та віброгасник з конічними пружинами, жорсткість яких регулюється шляхом стискання за допомогою преса. За допомогою коло-польового методу розроблено математичну та імітаційну модель електромагнітних та електромеханічних процесів у вібраторі. Для цього виконано числові розрахунки магнітного поля у вібраторі та на основі отриманих результатів визначено функціональні залежності між електромагнітною силою, магнітним потоком, магніторушійною силою та величиною повітряного зазору. Розроблено також модель механіки коливальної системи, процесів у приводі руху преса віброгасника та процесів у системі керування. Побудовані імітаційні моделі об'єднано в загальну модель у середовищі Simulink, за допомогою якої отримано часові діаграми процесів. Результати моделювання показали, що система забезпечує плавний перехід з однієї частоти вібрації на іншу, підтримуючи при цьому задану амплітуду коливань робочого органа та білярезонансний режим з високою енергетичною ефективністю. Бібл. 12, рис. 10, табл. 3.

Ключові слова: електромагнітний привод; вібраційний пристрій; керований віброгасник; автоматичне керування.

Надійшла 16.02.2023
Остаточний варіант 23.03.2023